Studies in Surface Science and Catalysis 130
A. Corma, F.V. Melo, S.Mendioroz and J.L.G. Fierro (Editors)

An Atomic XAFS study of the metal-support interaction in Pt/SiO_2-Al_2O_3 and Pt/MgO-Al_2O_3 catalysts: an increase in ionisation potential of platinum with increasing electronegativity of the support oxygen ions

D.C. Koningsberger[a], M.K. Oudenhuijzen[a], D.E. Ramaker[b] and J.T. Miller[c]

[a] Department of Inorganic Chemistry and Catalysis, Debye Institute, Utrecht University, PO Box 80083, 3508 TB Utrecht, The Netherlands
[b] Chemistry Department, George Washington University, Washington, DC 20052, USA
[c] Amoco Research Center, E-1F, 150 W. Warrenville Rd., Naperville, IL 60566, USA

The neo-pentane hydrogenolysis turn-over frequency (TOF) of platinum on macroporous acidic SiO_2-Al_2O_3 is about 500 times higher than that on basic MgO-Al_2O_3 hydrotalcite clay. The TOF increases with increasing electronegativity of the support oxygen ions similar to that found for Pt dispersed in microporous supports, such as LTL and Y zeolite. In addition, for Pt on silica-alumina, the intensity of the Fourier transform of the atomic XAFS oscillations, which were isolated from the XAFS spectra is larger and shifted to lower radius. A general model for the metal-support interaction is proposed, where a Coulomb attraction causes an increase in ionisation potential of the metal d-valence orbitals with increasing electronegativity (i.e. lower electron density) of the support oxygen ions.

1. INTRODUCTION

Numerous studies have reported enhancements in the specific reaction rates for benzene hydrogenation [1], propane hydrogenolysis [2] and neo-pentane hydrogenolysis and isomerization [3,4,5,6], on acidic supports compared to neutral supports. Several explanations for the metal-support interaction have been proposed in literature (i) Formation of a metal-proton adduct [3,7], (ii) Charge transfer between the metal atoms and the nearest neighbour zeolite oxygen atoms [8,9] and (iii) Polarisation of the metal particles by nearby cations [10,11]. For each explanation, however, there is experimental evidence, which is inconsistent with the proposed model [12]. Systematic experiments carried out by our group have shown that the catalytic activity and spectroscopic properties of supported noble metal catalysts are greatly affected by H^+ and K^+ in LTL zeolite [13] and by H^+, La^{+3}, different Si/Al ratio and non-framework Al in Y zeolite [12].

A newly developed tool called atomic XAFS (AXAFS), which is obtained from the X-ray Absorption Fine Structure (XAFS) spectra, can provide electronic information on metal-supported catalysts [14]. The intensity of the Pt AXAFS peak increases with increasing electronegativity of the support oxygen ions. The changes in the AXAFS data could be explained by an increase in the ionisation potential of platinum with increasing electronegativity of the zeolite oxygen ions

In this paper the metal-support interaction for platinum particles supported on high surface area, macroporous supports is further investigated. The electronegativity of the support oxygen ions was varied by using an amorphous acidic SiO_2-Al_2O_3 and a basic MgO-Al_2O_3 hydrotalcite clay. The influence of the support on the neo-pentane hydrogenolysis TOF of Pt was determined. XAFS spectroscopy (EXAFS and AXAFS) was used to investigate the structural and electronic properties of the supported Pt particles.

2. EXPERIMENTAL

2.1. Catalysts preparation

The supports were commercially available: SiO_2-Al_2O_3 (denoted by Si(Al)O), Davison grade 135, 510 m^2/g and 0.67 cc/g) and magnesium-alumina, hydrotalcite clay MgO-Al_2O_3 (denoted by Mg(Al)O), La Roche Ind, Inc, 166 m^2/g and 0.18 cc/g). The supports were calcined at 500°C and 550°C, respectively, for 16 hr. Platinum was added to each support by impregnation with $[Pt(NH_3)_4](NO_3)_2$ (Pt loading 2 wt%). The catalysts were dried at 120°C, calcined at 250°C and reduced in flowing hydrogen at 350°C. The Pt dispersions were determined by hydrogen chemisorption after reduction at 350°C and are given in Table 1.

Table 1. Dispersion and TOF values

Catalysts	Dispersion[1]	TOF[2]
SiO_2-Al_2O_3	0.85	2.7×10^{-2}
MgO-Al_2O_3	0.26	5.3×10^{-5}

[1] Determined by volumetric H_2 chemisorption assuming 1 H/Pt atom. [2]Molecules/sec-surface Pt atom.

2.2. Neo-pentane hydrogenolysis

Neopentane hydrogenolysis was conducted in a fixed bed reactor at 325°C, using 0.99 vol.% neo-pentane in H_2. The catalysts were re-reduced at 325°C for 1 hour, and conversion was adjusted to values less than 2.0% by varying the space velocity. The TOF was calculated based on H_2 chemisorption. The analysis of the reaction products was carried out using the Delplot method [15], which gives by extrapolation to zero conversion the primary product distribution.

2.3. XAFS data collection

X-ray absorption spectra have been collected at station 9.2 of the Daresbury SRS. The samples were pressed into self-supporting wafers and were then mounted in an in-situ cell equipped with Be windows. The EXAFS samples were reduced in flowing hydrogen at 400°C (heating rate 5°C/min) for 1 hour and evacuated at 200°C for 1 hour. XAFS spectra were recorded at liquid nitrogen temperature maintaining a vacuum of better than 2×10^{-3} Pa.

2.4. XAFS data-analysis methods

By using newly defined criteria the smooth atomic background and multi electron excitations are isolated from the AXAFS and EXAFS contributions (for further details see [16]). Theoretical phase and backscattering amplitudes for the Pt–Pt and Pt–O absorber-backscattering pairs were generated utilising the FEFF7 [17] code and calibrated against reference compounds [16]. The new references can be used from a k-value of about 2.5 $Å^{-1}$, significantly lower than the previously used experimental references. The result is a much

better isolation of the AXAFS peak at low *R*. Fitting is done in R-space, without Fourier filtering of the data. To analyse the metal-oxygen contribution to the spectra the difference file technique was used [12]. After subtracting the first metal-metal and metal-oxygen contributions, the remaining signal will be the AXAFS together with the higher order shells.

2.5. AXAFS

The AXAFS, $\chi_{AX}(k)$, is caused by the scattering of the photoelectron off the deep valence electrons in the periphery of the absorbing atom [14]. The well-known muffin-tin approximation can be used to approximate the embedded atom potential. As illustrated in Figure 1, the muffin-tin approximation "clips" the exact potential at the muffin-tin radius R_{mt} and sets it equal to the interstitial potential V_{int} [14]. Inside R_{mt} the potential is assumed to be spherical, outside it is assumed to be flat and zero (i.e. no forces are exerted on the particle in the interstitial region). V_{int} is determined by averaging the potential at R_{mt} of all the atoms in the cluster, and this determines the zero of energy or the effective bottom of the conduction band. A phase corrected and k weighted Fourier transform of $\chi_{AX}(k)$ leads to [14]: $|FT(ke^{-2i\delta}\chi_{AX})| \approx \Delta V^{*}\Gamma$ where $\Delta V = V_{emb} - V_{TFA}$ with V_{emb} the embedded atom potential, V_{TFA} the truncated free atom potential, and Γ a broadening function due to the limited Fourier transform range. The embedded potential reflects the electron distribution after embedding the free atom into its chemical environment and allowing interaction with its neighbours. This means that the FT directly reflects this change in the chemical environment. More specifically, the shape and intensity of the $|FT|$ can be represented by the shaded area between V_{free} and V_{emb} and below V_{cut} ($V_{cut} = 2\times V_{int} + |E_f|$) as illustrated in Figure 1 (For further details see [12,14]).

3. RESULTS

3.1. Neo-pentane hydrogenolysis

The results for conversion of neo-pentane are given in Table 1. Analysis of reaction products by the Delplot method indicated that methane, iso-butane (hydrogenolysis), and iso-pentane (isomerization) were primary products. It can be seen in Table 1 that the TOF of Pt particles supported on the acidic Si(Al)O is about 500 times higher than for Pt supported on the basic Mg(Al)O.

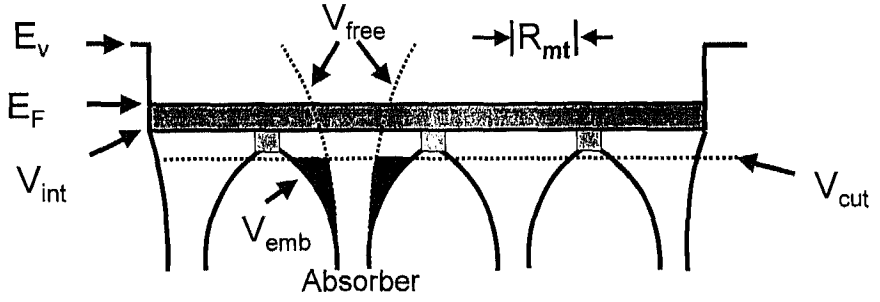

Fig. 1. Illustration of the muffin tin approximation to the interatomic potentials showing locations of E_v, E_F, V_{int}.

3.2. EXAFS

In Figure 2 the Fourier transform (k^2, Δk = 2.5 – 14 Å^{-1}) of the raw XAFS data (solid line) of the Pt/Si(Al)O sample is displayed. The shoulders at both the low and high R side of the first Pt-Pt peak in the Fourier transform are due to the non-linear Pt-Pt phase shift and the k dependence of the backscattering amplitude. Fitting of the experimental spectra was done in R-space over the range R = 1.6 to 3.1 Å using a k^2 weighted Fourier transform over the range Δk = 2.5 to 14.0 Å^{-1}.The results of the fit are shown in Figure 2 (dotted line). The EXAFS co-ordination parameters for both catalysts are given in Table 2.

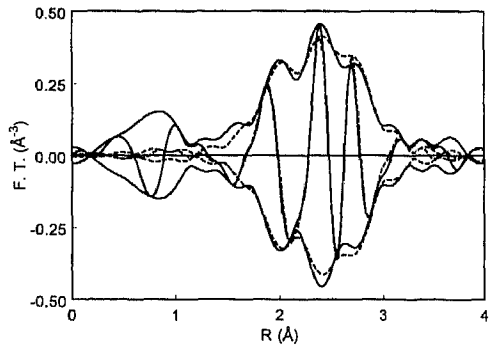

Fig. 2. Fourier Transform (k^2, Δk=2.5-14 Å^{-1}) of raw EXAFS data of Pt/Si(Al)O (solid line) and fit (dotted line).

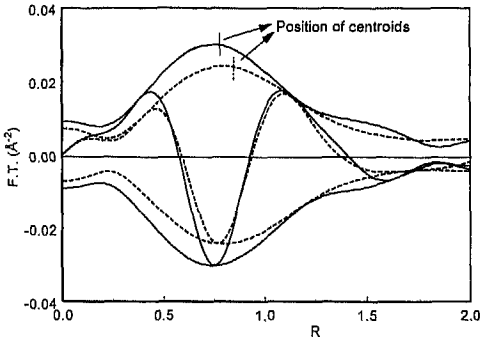

Fig. 3. Fourier Transform (k^l, Δk=2.5-8 Å^{-1}) of AXAFS data of Pt/Si(Al)O (solid line) and Pt/Mg(Al)O (dotted line).

3.3. AXAFS

It can clearly be seen in Figure 2 that at low values of R differences are present between fit and experimental data. These differences are due to the AXAFS contribution. Subtracting the calculated Pt-Pt and Pt-O contributions from the raw XAFS produces a difference file, which contains the AXAFS contribution. The k^l weighted Fourier transform of this difference file is given in Figure 3 for Pt/Si(Al)O (solid line) and for Pt/Mg(Al)O (dotted line). The amplitude of the AXAFS peak is larger and the centroid is at lower values of R for the Pt/Si(Al)O sample.

4. DISCUSSION

4.1. Neo-pentane hydrogenolysis

Since neo-pentane can not form an alkene intermediate, hydrogenolysis is dependent on only the catalytic activity of the metal [18,19] as confirmed by the primary reaction products: methane, iso-butane (hydrogenolysis), and iso-pentane (isomerisation). Moreover, neo-pentane does not undergo protolytic cracking at the temperatures used for the catalytic reaction (325°C). The protons present on the Si(Al)O support, therefore, do not contribute to the neo-pentane conversion. Hydrogenolysis reactions are dependent on the metal particle

Table 2. EXAFS co-ordination parameters

Coordination	Pt-Pt				Pt-O			
Parameters	N	R (Å)	$\Delta\sigma^2$ (Å^2)	E_0 (eV)	N	R (Å)	$\Delta\sigma^2$ (Å^2)	E_0 (eV)
Pt/Si(Al)O	6.7	2.67	0.007	3.1	0.1	2.13	0.000	3.1
Pt/Mg(Al)O	7.3	2.71	0.006	2.2	0.1	2.07	-0.003	5.3

size, generally, decreasing with increasing particle size: TOF identical for catalysts with a dispersions from about 0.1 to 0.7, but a factor 2 decrease as the dispersion increased to 1.0. Thus, at an equivalent dispersion, the TOF of Si(Al)O would increase to about 1000 times higher than that of Mg(Al)O. While the particle size does influence the rate, it is not sufficient to account for the large differences in TOF in these catalysts. We conclude that the change in TOF is primarily due to the metal-support interaction consistent with previous studies [12,14].

4.2. Structure of the Pt particles.

The metal particles in both Pt/Si(Al)O and Pt/Mg(Al)O catalysts have first shell Pt-Pt co-ordination numbers around 7; i.e. the average metal particle consists of approximately 40 atoms assuming a spherical particle morphology. A Pt-Pt coordination number of 6.7 for Pt/Si(Al)O is slightly larger than expected for a catalyst with a dispersion of 0.85 and may be due to the higher reduction temperature in the EXAFS measurements. A small interfacial oxygen contribution (only Pt atoms in the metal-support interface have oxygen neighbours) is detected within the first co-ordination sphere of Pt, but neither silicon, nor aluminum ions were found within 3 Å of the platinum particles for either catalyst. Because to the small Pt-O contribution to the EXAFS, the differences in the Pt-O distances are likely not significant. Since the Pt particles in both catalysts have the same structural properties, we conclude that the change in the catalytic properties of the metal particles is due to a change in their electronic properties induced by a Coulombic interaction with the oxygen ions of the support.

4.3. Nature of the metal-support interaction

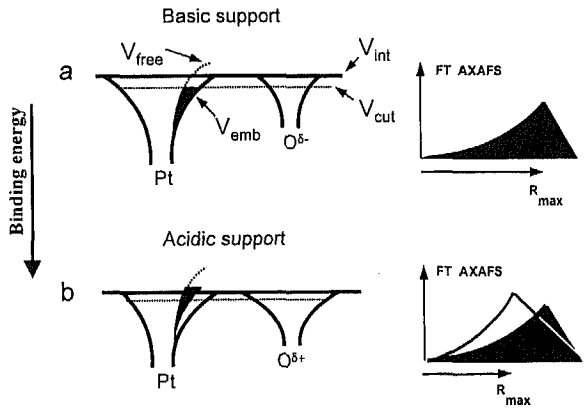

Fig. 4. Schematic potential curves for a basic (a) and acidic support (b) assuming polarisation of the cluster by the support.

For Pt/Si(Al)O, the intensity of the AXAFS peak is larger and the centroid is shifted to lower *R* in comparison to Pt/Mg(Al)O (see Figure 3). These results are consistent with the results recently published by our group for Pt/LTL [6] and Pt/Y [12]. The support properties (acidity, basicity) determine through the Madelung potential the electronegativity of the support oxygen ions. Figure 4a and b compare the difference in the Pt-O interatomic potential as the charge (electronegativity) on

the oxygen ion increases. The AXAFS peak in the Fourier transform of the Pt/Mg(Al)O data is schematically represented on the right side of Figure 4a with the black area and is determined by the difference between V_{free} and V_{emb}: the black area on the left side of Figure 4a. Increasing the charge on the oxygen (δ^+: higher electronegativity) will change the shape of the potential of platinum since the interaction with oxygen will move platinum electrons nearer to the oxygen. This is illustrated in Figure 4b by the larger Coulomb tail on the O atom with increased charge, and hence more "roll over" of the interatomic potential and the lowering of V_{cut}. This causes a larger difference between V_{emb} and the free atom potential as is shown on the left side of Figure 4b. The original difference (black area, in size and position) for the Pt/Mg(Al)O sample is given as a comparison. This larger difference causes an increase in the amplitude of the Fourier transform of the AXAFS oscillations and a shift of the centroid to lower R values as shownon the left side of Figure 4b. At the same time the platinum valence d orbitals are moved to higher binding energy; i.e. the ionisation potential of Pt is increased. Moreover, the Pt d-orbitals are radially contracted and the width of the d-band is reduced resulting in less "metallic" character. This is also reflected in the XPS 3d core level shift of Pd particles dispersed in LTL [6] and in the increase in the linear/bridge ratio of the CO FTIR spectra of Pd/LTL, Pt/LTL and Pt/SiO_2. [5].

The AXAFS studies on Pt/LTL [13], Pt/Y [12] and the results presented in this paper on Pt/Si(Al)O and Pt/Mg(al)O suggest a general model for the metal-support interaction, which is based upon a Coulomb attraction between the support oxygen ions and the platinum metal particles. An increase in electronegativity of the support oxygen ions leads to an increase in the ionisation potential of the platinum metal atoms. This change in binding energy of the metal valence orbitals alters the adsorptive, catalytic and spectroscopic properties of the metal particles. This model also implies that there is no transfer of electron density between the support and the metal particles.

REFERENCES

1. S.D. Lin, M.A. Vannice, J. Catal. 143 (1993) 539.
2. J.T. Miller, F.S. Modica, B.L. Meyers, D.C. Koningsberger, Prep. ACS Div. Petr. Chem. 38 (1993) 825.
3. Z. Karpinski, S.N. Gandhi, W.M.H. Sachtler, J. Catal. 141 (1993) 337.
4. S.T. Homeyer, Z. Harpinski, W.M.H. Sachtler, J. Catal. 123 (1990) 60.
5. B.L. Mojet, M.J. Kappers, J.T. Miller, D.C. Koningsberger, Proc. of the 15th Int. Cong. Catal., Baltimore, MD, (1996).
6. B.L. Mojet, M.J. Kappers, J.C. Meyers, J.W. Niemantsverdriet, J.T. Miller, F.S. Modica, D.C. Koningsberger, Stud. Surf. Sci. Catal. 84 (1994) 909.
7. Z. Zhang, T.T. Wong, W.M.H. Sachtler, J. Catal. 128 (1991) 13.
8. G. Larsen, G.L. Haller, Catal. Lett. 3 (1989) 103.
9. A. de Mallmann, D. Barthoumeuf, J. Chem. Phys. 87 (1990) 535.
10. A.P. Jansen, R.A. van Santen, J. Phys. Chem. 94 (1990) 6764.
11. E. Sanchez-Marcos, A.P.J. Jansen, R.A. van Santen, Chem. Phys. Lett. 16 (1990) 399.
12. D.C. Koningsberger, J. de Graaf, B.L. Mojet, D.E. Ramaker and J.T. Miller, Appl. Catal, in print.
13. B.L. Mojet, J.T. Miller, D.E. Ramaker and D.C. Koningsberger, J. Catal. 186 (1999) 373.
14. D.E. Ramaker, B.L. Mojet, W.E. O' Grady and D.C. Koningsberger, J. Phys. Condens. Matter. 10 (1998) 1.
15. N.A. Bhore, M.T. Klein, K.B. Bischoff, Ind. Eng. Chem. Res. 29 (1990) 313.
16. G.E. van Dorssen, D.E. Ramaker, D.C. Koningsberger, submitted Phys. Rev. B
17. S. I. Zabinsky, J. J. Rehr, A. Ankudinov, R. C. Albers, M. J. Eller, Phys. Rev. B 52 (1995) 2995.
18. S.M. Davis, G.A. Somorjai, *The chemical physiscs of solid surfaces and heterogeneous catalysts* (D.A. King, D.P. Woodruff, eds.), Elsevier Publishers Amsterdam, 4 (1982) 271.
19. J.R. Anderson, N.R. Avery, J. Catal. 16 (1967) 315.